

## Observation of Autoionization Suppression through Coherent Population Trapping

N. E. Karapanagioti, O. Faucher, Y. L. Shao, and D. Charalambidis

*Foundation for Research and Technology-Hellas, Institute of Electronic Structure and Laser, P.O. Box 1527, 711 10 Heraklion, Crete, Greece*

H. Bachau and E. Cormier

*Laboratoire de Collisions Atomiques, CNRS-UPR 260, Université Bordeaux I, 351 Cours de Libération, 33405 Talence Cedex, France*

(Received 4 October 1994)

The strong electromagnetic coupling of two autoionizing states is experimentally investigated for the first time and is shown to lead to coherent population trapping resulting in a reduction of the ionization. The experimental observation of partial stabilization is supported by a theoretical analysis which reproduces the modification of the Fano profiles and indicates that the strong coupling of the two states leads to the trapping of the population in the ground state of the atom.

PACS numbers: 32.80.Dz

The purpose of this paper is to report the observation of partial stabilization in an atomic system where reduction of ionization occurs as a result of coherent population trapping. The trapping is achieved through the strong electromagnetic coupling of two autoionizing states (AIS), one of which is probed through a second electromagnetic field.

The modification of autoionizing states due to coherent coupling with each other has been the subject of several theoretical studies in the last ten years [1,2]. However, despite the promising features predicted by the theory, there have been no experimental studies of these effects to our knowledge. The coupling of two autoionizing states is therefore a new and inviting issue to be addressed in this context. The manipulation of states lying high above the ionization threshold is also of major interest, concerning coherent sources of very short wavelength. Only recently, experiments performed in  $\Lambda$  systems involving two bound states have demonstrated the possibility of modifying an AIS either through laser induced transparency [3] or through laser induced continuum structure [4]. However, since previous work always involved the coupling of an AIS to a bound state (below the threshold), how far one went up in the continuum was limited by the frequency of the coupling field. The coupling of two autoionizing states, apart from the theoretical interest it presents, allows the transfer of the coupled system to much higher energies above the threshold.

In the present work, we studied a ladder system with two autoionizing states coupled to each other. The probing of the lower state through a weak electromagnetic field revealed strong modifications of the autoionizing line shape depending on the detuning of the dressing field. A theoretical analysis based on the density matrix formalism and including the spatiotemporal structure of the laser pulse indicated the occurrence of population trapping in the ground state of the atom.

The scheme employed in this experiment made use of a strong laser field to couple the broad  $3p^2\ ^1S_0$  AIS of magnesium ( $\Gamma = 280\text{ cm}^{-1}$  [5]) to the higher lying,

narrow  $3p3d\ ^1P_1$  autoionizing state. The  $3p^2$  is excited from the ground state through a two-photon transition achieved by a much weaker laser, which can therefore be considered as a probe. The photons and couplings involved are shown schematically in Fig. 1, including the ionization widths of the autoionizing states ( $\Gamma_a, \Gamma_b$ ) and that of the ground state through two-photon absorption to the continuum ( $\gamma_g$ ).

The experiment was conducted using two tunable linearly polarized pulsed dye lasers (Lambda Physik LPD3000) that were simultaneously pumped by a XeCl excimer laser (Lambda Physik LPX300). The lasers provided pulses in the visible of  $\sim 12$  ns duration and  $\sim 5$  mJ energy. The probe laser output was frequency doubled using a BBO frequency doubling crystal to produce radiation between 289 and 298 nm, with an energy of  $\sim 0.5$  mJ. The frequency doubled output was then attenuated by a factor of 10 and the two laser beams were combined using a dichroic mirror. They were then directed to the vacuum chamber ( $P \leq 2 \times 10^{-6}$  mbar) and were focused on the magnesium beam by a 5 cm focusing lens. Since the lens was not achromatic, the focus positions of the beams were adjusted to coincide by the use of two telescopes, employing two 10 cm focusing lenses

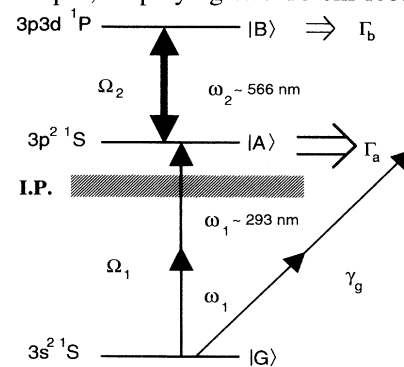


FIG. 1. Partial energy level diagram of magnesium indicating the scheme used and the couplings involved in the excitation.

each, resulting in a magnification  $M \cong 1$ . The distance between the lenses was adjusted for maximum coincidence of the beams in the interaction region.

The magnesium was heated in an oven to  $\sim 410^\circ\text{C}$ , came out through a 1 mm aperture, and was collimated at right angles to the laser beams. The number density of the beam in the interaction region was of the order of  $10^9$  atoms/cm<sup>3</sup>. Upon ionization of the magnesium atoms from the uv laser, the ions were repelled by a metallic plate kept at a positive potential of  $\sim 300$  V towards a short time-of-flight mass spectrometer, equipped with a two-stage microchannel plate detector. An entrance slit was used in order to confine the detection volume around the focus. The signal from the microchannel plates was fed into a preamplifier and from there to an amplifier and to a computer.

The intensities of the lasers at the focus point were estimated within a factor of 4 to be  $I_1 \sim 10^8$  W/cm<sup>2</sup> for the probe laser and  $I_2 \sim 10^{10}$  W/cm<sup>2</sup> for the dressing laser. This uncertainty is mainly related to the accuracy in the measurement of the beam size. Although the beams were aligned for maximum overlap in the interaction region, the overlap was not total due to the different beam waists, wavelengths, and varying divergences introduced by the telescopes. We therefore have to assume that, superimposed on our signal, there was a steady background arising from ionization from the probe laser in a volume where the dressing laser was weak.

The data obtained were of two types: (a) by keeping the wavelength  $\lambda_2$  of the dressing laser constant and scanning the probe wavelength  $\lambda_1$  and (b) by scanning  $\lambda_2$  and keeping  $\lambda_1$  constant. The absolute value of the laser wavelength was known to within 0.2 nm and the laser bandwidth was  $\sim 0.2$  cm<sup>-1</sup>. Initial scans of the  $3p^2$  AIS were performed at the reported probe laser intensity to ensure that the resonance was not saturated.

The data in Fig. 2(a) show the structure induced in the broad  $3p^2$  AIS. Near the center of the resonance (top figure), the induced structure is a nearly symmetric dip leading to an ionization reduction of around 30%. For a detuning of 6.8 nm (bottom figure), the induced autoionizinglike structure appears much more asymmetric on the side of the AIS feature at the wavelength that satisfies the energy balance of the process. As can be seen by comparison with single-color spectra of the  $3p^2$  state (indicated by the dashed line), the induced structure displays a distinct autoionizinglike behavior in both cases by resulting in both reduction and increase of the ionization in the manner of a Fano profile. This behavior is mirrored in the scans of the dressing laser  $\lambda_2$  with the probe laser fixed at the center and at the wings of the resonance, respectively. The rather symmetric dip observed in the top of Fig. 2(b) becomes an asymmetric profile when  $\lambda_1$  is detuned away from the peak of the  $3p^2$  AIS (bottom figure). Changing the sign of the detuning, an asymmetry reversal of the induced structure has been

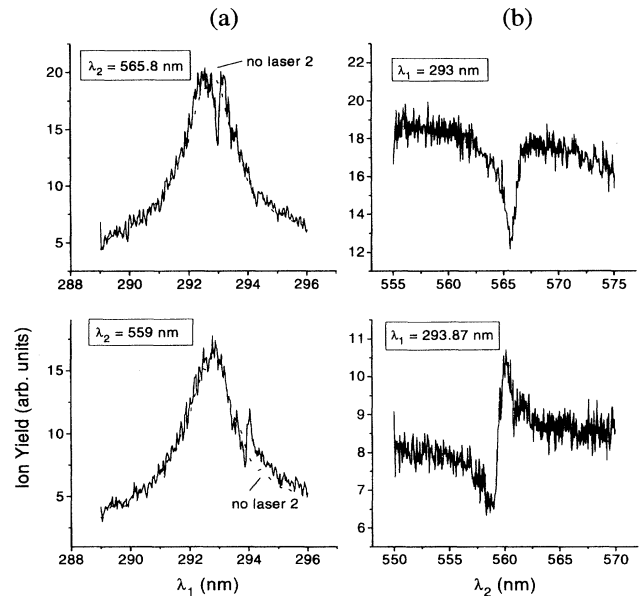


FIG. 2. Data obtained (a) by scanning the probe laser with the dressing laser wavelength fixed, and (b) by scanning the dressing laser with the probe laser wavelength fixed. Each pair of scans ( $\lambda_1, \lambda_2$ ) corresponds to the resonance condition  $2\omega_1 + \omega_2 = E_{|3p3d\rangle}$ . The dashed line indicates the spectra of the  $3p^2$  state obtained without the dressing laser.

observed. The degree of the asymmetry depends on the magnitude of the detuning. A more thorough analysis of the behavior of the asymmetry around the resonance will be the subject of a longer paper.

In order to provide theoretical insight into the above observations, we developed a model that incorporates the states and the dominant mechanisms relevant to our problem. While atomic structure and dynamical calculations will be given in detail in a future paper, we will briefly expose our approach here. A configuration interaction method was applied for the representation of the Mg states, and, in the particular case of the  $3p^2$  and the  $3p3d$  autoionizing states, a partition of the space was performed within the framework of the Feshbach [6] formalism. Using appropriate  $P$  and  $Q$  projection operators, we represented these resonances as quasibound states embedded in a continuum. The notations  $3p^2$  and  $3p3d$  now refer to this quasibound part. This approach, first proposed by Lambropoulos and Zoller [1] in the context of multiphoton processes (see Ref. [2] for an application in helium), is of great help in the development of dynamical equations and leads naturally to the definition of the positions, widths, Fano  $q$  parameters, and relevant dipole couplings. In order to provide an analysis that includes the temporal and spatial dependences of the two fields, we formulate the problem in terms of a set of density matrix equations. After elimination of the continua, we are left with six coupled equations governing the time evolution of the populations

$\rho_{11}(t)$ ,  $\rho_{22}(t)$ , and  $\rho_{33}(t)$  of states  $3s^2$ ,  $3p^2$ , and  $3p3d$ , respectively,

$$\begin{aligned}\frac{d\rho_{11}}{dt} &= -\gamma_g \rho_{11} + 2\text{Im}[\Omega_1(1 - i/q)\rho_{21}], \\ \frac{d\rho_{22}}{dt} &= -\Gamma_a \rho_{22} - 2\text{Im}[\Omega_1(1 + i/q)\rho_{21}] + 2\text{Im}(\Omega_2 \rho_{32}), \\ \frac{d\rho_{33}}{dt} &= -\Gamma_b \rho_{33} - 2\text{Im}(\Omega_2 \rho_{32}), \\ \frac{d\rho_{21}}{dt} &= -[-i\delta_1 + (\gamma_g + \Gamma_a)/2]\rho_{21} - i\Omega_1[(1 - i/q)\rho_{11} - (1 + i/q)\rho_{22}] - i\Omega_2 \rho_{31}, \\ \frac{d\rho_{31}}{dt} &= -[-i(\delta_1 + \delta_2) + (\gamma_g + \Gamma_b)/2]\rho_{31} - i\Omega_2 \rho_{21} + i\Omega_1(1 + i/q)\rho_{32}, \\ \frac{d\rho_{32}}{dt} &= -[-i\delta_2 + (\Gamma_a + \Gamma_b)/2]\rho_{32} - i\Omega_2(\rho_{22} - \rho_{33}) + i\Omega_1(1 + i/q)\rho_{31}.\end{aligned}\quad (1)$$

In the above equations, we recognize the atomic parameters and couplings terms given in Fig. 1. Note that the two-photon matrix element  $\Omega_1$  couples the states  $3s^2$  and  $3p^2$  and is proportional to the intensity  $I_1$  of the probe laser;  $\Omega_2$  couples  $3p^2$  to  $3p3d$  and is proportional to the square root of the dressing laser intensity  $I_2$ . The width  $\gamma_g$  behaves like  $I_1^2$  and is associated to ionization to the  $3sks$  and  $3skd$  continua and  $q$  is the Fano parameter associated to the  $3p^2$  resonance. There is no such parameter for the very narrow  $3p3d$  resonance due to the fact that we neglected the dipole transitions between the two resonant states and the  $3skl$  continua. Indeed, since such dipoles are due to correlations [2], they are expected to be small compared to the direct strong  $\Omega_2$  dipole (where the  $3p$  orbital is shared). The detunings are defined as follows:  $\delta_1 = 2\hbar\omega_1 - (E_g - E_a)$  and  $\delta_2 = \hbar\omega_2 - (E_a - E_b)$ , where  $E$  denotes the respective state energies. The different parameters are listed in Table I. Since polarization effects have been neglected in the atomic structure calculation, we used accurate experimental or theoretical values (when available) for the positions and lifetimes of the states involved. We used  $\cosh^{-1}$  and Gaussian shapes for the temporal and spatial dependence of the pulses, respectively. According to experimental conditions the interaction time was about  $10^{-8}$  s.

The theoretical results are given in Figs. 3(a) and 3(b) for situations corresponding to the experimental cases shown in Figs. 2(a) and 2(b). We note an overall agreement between theory and experiment, particularly when the peaks and dips are clearly pronounced (at the same positions) in both sets of figures. What we see, in fact, is

a transition from single peak to a two-peak curve which reflects the ac Stark splitting of the transition due to the strong field  $\Omega_2$ . This has been the subject of flourishing literature but, to our knowledge, this is the first time that such splitting is clearly observed and quantified in the case of two autoionizing resonances. We note the presence of the dip induced on the autoionization profile which reflects a stabilization of the system. Indeed, we see in Figs. 2(a) and 3(a) that there are no dips when laser 2 is off. Stabilization occurs in *all* cases when  $\delta_1 + \delta_2 = 0$ , and it corresponds to a situation of the coherent trapping [7] encountered in  $\Lambda$ -type systems. This has been noticed by Lami, Rahman, and Spizzo [8] in a similar three-level system (for helium) but never observed in the context of two autoionizing resonances. The conditions under which stabilization occurs are now precise: The intensity  $I_1$  is such that the first transition, from the ground state to the  $3p^2$  state, occurs in the weak field regime where an ionization rate can be defined. On the other hand, there is a “strong” coherent mixing between the  $3p^2$  and  $3p3d$  resonances in the sense that the dipole coupling  $\Omega_2$  is strong enough to “compete” with the autoionizing width  $\Gamma_a$ . We plotted, in Fig. 4(a), the ionization signal versus the intensity  $I_2$  with  $\delta_1 + \delta_2 \approx 0$ . Stabilization begins when the dipole value reaches the order of magnitude of the autoionizing width that is at about  $5 \times 10^8$  W/cm<sup>2</sup>. In order to illustrate that the quastabilization arises from population trapping, we also plotted, in Fig. 4(b), the population of the ground state ( $\rho_{11}$ ) for  $\lambda_1 = 293$  nm. In the region of the dip [see

TABLE I. The intensities  $I_1$  and  $I_2$  are given in atomic units (1 a.u. =  $14.04 \times 10^{16}$  W/cm<sup>2</sup>). The energies  $E_a$  and  $E_b$  are the excitation energies of the  $3p^2$  and  $3p3d$  states, respectively.

$q$	$\Gamma_a^{(a)}$	$\Gamma_b^{(b)}$	$\Omega_1$	$\Omega_2$	$E_a^{(a)}$	$E_b^{(c)}$
25	0.001 27 au	0.000 06 au	$665I_1$ au	$2.2I_2^{1/2}$ au	8.464 eV	10.65 eV
$\gamma_g \sim 10^8 I_1^2$ au						

<sup>(a)</sup>Y. L. Shao, C. Fotakis, and D. Charalambidis, Phys. Rev. A **48**, 3636 (1993).

<sup>(b)</sup>T. N. Chang, Phys. Rev. A **34**, 4554 (1986).

<sup>(c)</sup>G. Mehlman-Balloffett and J. M. Esteve, Astrophys. J. **157**, 945 (1969); W. C. Martin and R. Zalubas, J. Phys. Chem. Ref. Data **9**, 1 (1980).

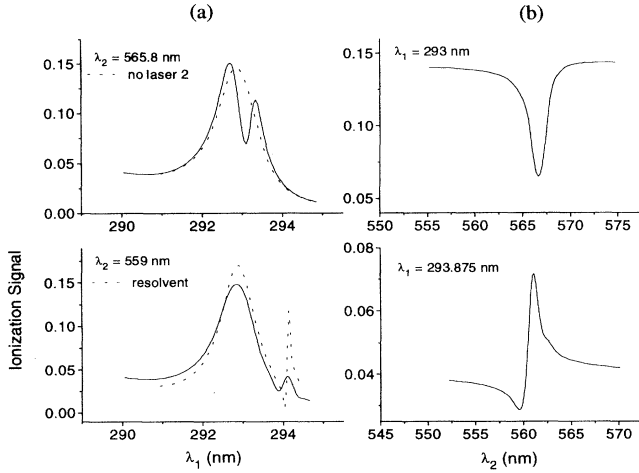


FIG. 3. Theoretical ionization signal obtained by (a) scanning the probe laser with the dressing laser fixed. The upper figure also shows the ionization signal obtained without dressing laser (dashed line). The lower figure includes the ionization signal calculated with Eq. (2) and divided by 2.5 (dashed line). (b) Signal obtained by scanning the dressing laser with the probe laser fixed. The laser intensities are  $I_1 = 10^8 \text{ W/cm}^2$  and  $I_2 = 0.25 \times 10^{10} \text{ W/cm}^2$ , respectively, at the peak of the pulses.

Fig. 3(b)], the population of the ground state increases, thus resulting in a decrease of the ionization.

It is not possible to extract an analytical formula from Eq. (1), but for square pulses this can be done on the basis of resolvent operator equations and under weak field conditions [1]. In the context of our problem ( $q \gg 1$ ,  $\Gamma_b \ll \Gamma_a$ , and  $\gamma_g \ll \Gamma_a \leq \Omega_2$ ) we found that the total ionization rate is approximated by

$$\frac{dP}{dt} \approx \gamma_g + \Gamma_a \times \frac{\Omega_1(\delta_1 + \delta_2)^2}{[\delta_1(\delta_1 + \delta_2) - \Omega_2^2]^2 + (\Gamma_a^2/4)(\delta_1 + \delta_2)^2}. \quad (2)$$

We recognize, in the above formula, the two channels for ionization: the direct two-photon absorption with rate  $\gamma_g$  and the indirect one which may be interpreted as the product of the percentage of population in the modified  $3p^2$  (which reflects the effect of coherent mixing between the two resonances) by its autoionizing rate  $\Gamma_a$ . When  $\delta_1 + \delta_2 = 0$ , the second channel cancels and more population is trapped in the ground state, thus giving rise to the experimental dip.

We reported, in Fig. 3(a), the ionization signal calculated with Eq. (2) and, save for a normalization factor, the overall features of the density matrix curve are well represented. We note that the structures are much more pronounced in the case of a square pulse. This illustrates the importance of the pulse parameters and spot overlap for an accurate modeling of the experiment.

To conclude, we have studied experimentally the modification of two autoionizing states coupled to each other through a strong electromagnetic field. We have observed

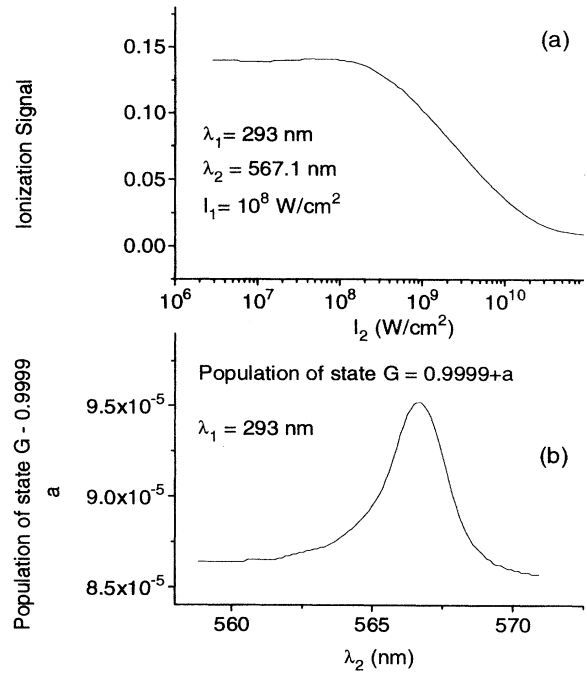


FIG. 4. (a) Theoretical ionization signal obtained with probe and dressing lasers fixed and  $\delta_1 + \delta_2 \approx 0$  versus the intensity of the dressing laser. (b) Mean value of the ground state population versus the coupling laser wavelength.

a reduction of ionization and profile changes arising from such a coupling. The theoretical analysis presented has demonstrated that the phenomena reported are indeed due to the coherent interaction between the autoionizing states, which leads to partial stabilization and population trapping in the ground state. This effect occurs when the dipole coupling between the two states is strong enough to compete with the main autoionization decay channel through the broad AIS.

This study indicates novel ways to modify continuum structure by appropriate tuning of the wavelength and intensity of a coupling laser, opening up the field of coherent interactions high up into the continuum.

- [1] P. Lambropoulos and P. Zoller, Phys. Rev. A **24**, 379 (1981).
- [2] H. Bachau, P. Lambropoulos, and Robin Shakeshaft, Phys. Rev. A **34**, 4785 (1986).
- [3] K.-J. Boller, A. Imamoglu, and S.E. Harris, Phys. Rev. Lett. **66**, 2593 (1991).
- [4] O. Faucher, Y.L. Shao, D. Charalambidis, and C. Fotakis, Phys. Rev. A **50**, 641 (1994).
- [5] Y.L. Shao, C. Fotakis, and D. Charalambidis, Phys. Rev. A **48**, 3636 (1993).
- [6] H. Feshbach, Ann. Phys. (N.Y.) **19**, 287 (1962).
- [7] K. Shimoda, in *Laser Spectroscopy of Atoms and Molecules*, edited by H. Walther (Springer-Verlag, Berlin, 1976).
- [8] A. Lami, N.K. Rahman, and P. Spizzo, Phys. Rev. A **40**, 2385 (1989).